

THE X-RAY SPECTRAL PROPERTIES AND VARIABILITY OF LUMINOUS HIGH-REDSHIFT
ACTIVE GALACTIC NUCLEIO. SHEMMER,¹ W. N. BRANDT,¹ C. VIGNALI,^{2,3} D. P. SCHNEIDER,¹
X. FAN,⁴ G. T. RICHARDS,⁵ AND MICHAEL A. STRAUSS⁵*Received 2005 April 8; accepted 2005 May 20*

ABSTRACT

We perform a detailed investigation of moderate-to-high quality X-ray spectra of ten of the most luminous active galactic nuclei (AGNs) known at $z > 4$ (up to $z \sim 6.28$). This study includes five new *XMM-Newton* observations and five archived X-ray observations (four by *XMM-Newton* and one by *Chandra*). We find that the X-ray power-law photon indices of our sample, composed of eight radio-quiet sources and two that are moderately radio loud, are not significantly different from those of lower redshift AGNs. The upper limits obtained on intrinsic neutral hydrogen column densities, $N_{\text{H}} \lesssim 10^{22}–10^{23} \text{ cm}^{-2}$, indicate that these AGNs are not significantly absorbed. A joint fit performed on our eight radio-quiet sources, with a total of ~ 7000 photons, constrains the mean photon index of $z > 4$ radio-quiet AGNs to $\Gamma = 1.97^{+0.06}_{-0.04}$, with no detectable intrinsic dispersion from source to source. We also obtain a strong constraint on the mean intrinsic column density, $N_{\text{H}} \lesssim 3 \times 10^{21} \text{ cm}^{-2}$, showing that optically selected radio-quiet AGNs at $z > 4$ are, on average, not more absorbed than their lower-redshift counterparts. All this suggests that the X-ray production mechanism and the central environment in radio-quiet AGNs have not significantly evolved over cosmic time. The mean equivalent width of a putative neutral narrow Fe K α line is constrained to be $\lesssim 190 \text{ eV}$, and similarly we place constraints on the mean Compton reflection component ($R \lesssim 1.2$). None of the AGNs varied on short ($\sim 1 \text{ hr}$) timescales, but on longer timescales (months-to-years) strong variability is observed in four of the sources. In particular, the X-ray flux of the $z=5.41$ radio-quiet AGN SDSS 0231–0728 dropped by a factor of ~ 4 over a rest-frame period of 73 d. This is the most extreme X-ray variation observed in a luminous $z > 4$ radio-quiet AGN.

Subject headings: galaxies: active – galaxies: nuclei – X-rays: galaxies

1. INTRODUCTION

Active galactic nuclei (AGNs) at $z > 4$ are valuable cosmological probes of the physical environment in the ~ 1 Gyr old Universe, following the re-ionization epoch at the end of the ‘dark ages’ (e.g., Fan et al. 2002). Investigations of physical processes in these sources, and in particular their energy production mechanism, are important for understanding the ionizing flux contribution from AGNs in the early Universe, black hole (BH) growth, and the evolution of mass accretion in galactic nuclei (see Brandt & Hasinger 2005 for a recent review). It is not yet clear whether the small-scale physics of active nuclei are sensitive to the strong large-scale environmental changes the Universe has experienced since $z \approx 6$.

The penetrating X-ray emission from AGNs is of particular interest, since it allows one to probe the innermost region of the accretion flow, near the central supermassive BH. Until fairly recently, X-ray detections of $z > 4$ AGNs were limited to a handful of sources with poor photon statistics, preventing a detailed analysis of their X-ray spectral properties (Kaspi, Brandt, & Schneider 2000); this was also, in part, a consequence of the relatively small number ($\lesssim 100$) of such sources discovered by the year 2000. The past five years have seen a rapid increase in optical discoveries of $z > 4$ AGNs,

largely as a result of two surveys, the Palomar Digital Sky Survey (DPOSS; Djorgovski et al. 1998) and the Sloan Digital Sky Survey (SDSS; York et al. 2000), which have raised the number of such sources to ~ 600 (e.g., Schneider et al. 2005). A rapid increase in X-ray detections of $z > 4$ AGNs soon followed, with ~ 90 such sources to date.⁶ *Chandra* and *XMM-Newton* observations of these sources have provided constraints on their mean global X-ray spectral properties, in particular their photon index and intrinsic absorption column density (e.g., Brandt et al. 2004; Vignali et al. 2005). However, many of the X-ray observations are shallow, aimed at just detecting the AGN, and do not allow useful measurements of the spectral properties in individual sources (e.g., Brandt et al. 2002; Vignali et al. 2003a, 2005). Exposure times of several tens of ks with *Chandra* and *XMM-Newton* are needed to measure the spectral properties accurately. Such observations are important for investigating the energy production mechanism at this early epoch, and testing whether the X-ray spectral properties have evolved over cosmic time.

Recent studies of X-ray spectral properties and their dependence on redshift and luminosity have led to conflicting conclusions. For example, while Bechtold et al. (2003) reported that the X-ray photon indices (Γ) of $z > 4$ AGNs are *flatter* (1.5 ± 0.5) than those of nearby AGNs, Grupe et al. (2005) reported that their Γ are rather *steep* (2.23 ± 0.48). The first study was based upon a sample of 16 radio-quiet sources observed by *Chandra* with low total counts (see Table 1 of Bechtold et al. 2003), and one of their objects (SDSS J103027.10+052455.0, hereafter SDSS 1030+0524) is common with the present work. The second study was

¹ Department of Astronomy & Astrophysics, The Pennsylvania State University, University Park, PA 16802, USA; ohad@astro.psu.edu

² INAF - Osservatorio Astronomico di Bologna, Via Ranzani 1, 40127 Bologna, Italy

³ Dipartimento di Astronomia, Universita’ degli Studi di Bologna, Via Ranzani 1, 40127 Bologna, Italy

⁴ Steward Observatory, University of Arizona, 933 North Cherry Avenue, Tucson, AZ 85721, USA

⁵ Princeton University Observatory, Peyton Hall, Princeton, NJ 08544, USA

⁶ See <http://www.astro.psu.edu/users/niel/papers/highz-xray-detected.dat> for a regularly updated compilation of X-ray detections at $z > 4$.

TABLE 1
LOG OF *XMM-Newton* OBSERVATIONS

| AGN | z | α | δ | Galactic N_{H}^{a} (10^{20} cm^{-2}) | Obs. Date | Exp. Time (ks) / Total Counts | | | | Ref. |
|-----------------------------|------|------------|-------------|---|--------------|-------------------------------|------------|-------------|---|------|
| | | (J2000.0) | (J2000.0) | | | MOS1 | MOS2 | pn | | |
| New Observations | | | | | | | | | | |
| PSS 0121+0347 ^b | 4.13 | 01 21 26.2 | +03 47 06.3 | 3.23 | 2004 Jan 09 | 25.7 / 139 | 25.9 / 185 | 21.7 / 540 | 1 | |
| SDSS 0210–0018 ^b | 4.77 | 02 10 43.2 | –00 18 18.3 | 2.66 | 2005 Feb 05 | 18.7 / 112 | 18.7 / 117 | 16.5 / 594 | 1 | |
| SDSS 0231–0728 | 5.41 | 02 31 37.7 | –07 28 54.5 | 2.90 | 2004 Jan 07 | 31.6 / 70 | 31.6 / 101 | 27.7 / 309 | 1 | |
| PSS 0926+3055 | 4.19 | 09 26 36.3 | +30 55 04.9 | 1.89 | 2004 Nov 13 | 27.8 / 289 | 27.8 / 295 | 23.8 / 1156 | 1 | |
| PSS 1326+0743 | 4.17 | 13 26 11.8 | +07 43 57.5 | 2.01 | 2003 Dec 28 | 31.3 / 247 | 31.3 / 229 | 27.1 / 963 | 1 | |
| Archival Observations | | | | | | | | | | |
| Q 0000–263 | 4.10 | 00 03 22.9 | –26 03 17 | 1.67 | 2002 Jun 25 | 34.0 / 295 | 34.0 / 322 | 34.0 / 1229 | 2 | |
| BR 0351–1034 | 4.35 | 03 53 46.9 | –10 25 19 | 4.08 | 2002 Aug 23 | 17.9 / 31 | 17.9 / 15 | 15.1 / 166 | 3 | |
| SDSS 1030+0524 | 6.28 | 10 30 27.1 | +05 24 55 | 3.17 | 2003 May 22 | 44.3 / 80 | 43.9 / 81 | 43.4 / 333 | 4 | |
| BR 2237–0607 | 4.56 | 22 39 53.6 | –05 52 19 | 3.84 | 2003 May 17 | 17.2 / 60 | 17.3 / 76 | 16.3 / 306 | 5 | |

REFERENCES. — 1. This work; 2. Ferrero & Brinkman (2003); 3. Grupe et al. (2004); 4. Farrah et al. (2004); 5. Grupe et al. (2005)

^aGalactic absorption column densities from Dickey & Lockman (1990), obtained using the optical coordinates of the sources given in this Table and using the HEASARC N_{H} tool at <http://heasarc.gsfc.nasa.gov/cgi-bin/Tools/w3nh/w3nh.pl>

^bModerately radio-loud source.

based upon a sample of 16 sources (11 of which are radio quiet) observed with *XMM-Newton* with low-to-high total counts (see Table 1 of Grupe et al. 2005); four of those sources (Q 0000–263, BR 0351–1034, SDSS 1030+0524, and BR 2237–0607) are common with the present work, and we use the same X-ray data that were discussed in that study. The recent analysis by Vignali et al. (2005), which is based upon the joint X-ray spectral fitting of a sample of 48 $z > 4$ radio-quiet AGNs observed with *Chandra* in the redshift range 3.99–6.28, argues that the X-ray spectral properties of AGNs do not show any significant evolution or luminosity dependence. Our aim in this paper is to address this puzzle by uniformly analyzing a sample of moderate-to-high quality X-ray spectra of $z > 4$ AGNs, with ≈ 200 –1000 counts per source. In this paper, we consider radio-quiet and radio-loud AGNs separately, as radio-loud sources might exhibit X-ray emission from their jets. The X-ray properties of the two AGN sub-classes differ significantly from one another; for example, the X-ray spectra of radio-loud AGNs are flatter than those of radio-quiet sources (e.g., Wilkes & Elvis 1987; Cappi et al. 1997; Porquet et al. 2004) and, at high redshift, radio-loud AGNs show signs of higher intrinsic absorption (e.g., Worsley et al. 2004a, b) and larger X-ray variability (e.g., Fabian et al. 1999). Since radio-quiet sources represent the majority of luminous AGNs at all redshifts (e.g., Stern et al. 2000; Ivezic et al. 2002; Petric et al. 2003), our analysis focuses on the properties of this sub-class.

Moderate-to-high quality spectra of only five $z > 4$ radio-quiet AGNs have been obtained with *XMM-Newton* and *Chandra* over the past three years, with only one such source having more than 1000 counts (Q 0000–263, Ferrero & Brinkmann 2003; see also Farrah et al. 2004; Grupe et al. 2004; Schwartz & Virani 2004; Grupe et al. 2005). In this paper we almost double that number with new data from *XMM-Newton*, adding two more sources with over 1000 counts, and study the broad-band X-ray spectral properties of ten AGNs with an average redshift of 4.8. In § 2 we describe our five *XMM-Newton* observations, the data reduction, and the analysis. In § 3 we expand our original sample

by adding archived high-quality *XMM-Newton* and *Chandra* spectra of five $z > 4$ radio-quiet AGNs, and in § 4 we investigate the mean X-ray spectral properties of our radio-quiet sample. Our results are discussed in § 5 and summarized in § 6. Throughout the paper we use the standard cosmological model, with parameters $\Omega_{\Lambda}=0.7$, $\Omega_{\text{M}}=0.3$, and $H_0=70 \text{ km s}^{-1} \text{ Mpc}^{-1}$ (Spergel et al. 2003).

2. NEW HIGH-QUALITY SPECTRA OF $Z > 4$ AGNS

2.1. Observations and Data Reduction

We have obtained imaging spectroscopic observations of five $z > 4$ AGNs with *XMM-Newton* (Jansen et al. 2001). Three of the sources were discovered in the DPOSS survey and were detected in X-rays by Vignali et al. (2003a); two were discovered in the SDSS survey and detected in X-rays by Vignali et al. (2001, 2003b). Three of the sources are radio quiet with an upper limit on the radio flux, while two, PSS 0121+0347 and SDSS 0210–0018, are moderately radio loud, following the classification of Kellermann et al. (1989), and have $R=300$ and $R=80$, respectively (Vignali et al. 2003a, 2001). These five sources were among the X-ray brightest of a sample of $z > 4$ AGNs previously targeted with *Chandra* snapshot ($\lesssim 10$ ks) observations (Vignali et al. 2001, 2003a, b). One of these sources, SDSS 0231–0728 at $z=5.41$ (Anderson et al. 2001), is the highest redshift AGN detected with the automated SDSS detection algorithm. The short, higher angular resolution *Chandra* observations allow prediction of the number of counts expected from the *XMM-Newton* observations, and they eliminate the possibility of significant source confusion due to the lower angular resolution of *XMM-Newton*. No nearby contaminating sources were detected in the *Chandra* images of our five AGNs.

A log of the new *XMM-Newton* observations appears in Table 1 (first five sources). The data were processed using standard SAS⁷ v6.1.0 and FTOOLS tasks. The event files of all the observations were filtered to include

⁷ *XMM-Newton* Science Analysis System. See http://xmm.vilspa.esa.es/external/xmm_sw/cal/sas_frame.shtml

TABLE 2
BEST-FIT X-RAY SPECTRAL PARAMETERS

| AGN | N_{H}^{a} | Γ | $f_{\text{E}}(1 \text{ keV})^{\text{b}}$ | $\chi^2(\text{DOF})$ |
|----------------|---------------------------|------------------------|--|----------------------|
| PSS 0121+0347 | ≤ 2.91 | $1.81^{+0.16}_{-0.16}$ | $7.64^{+0.96}_{-1.01}$ | 54.8(52) |
| SDSS 0210-0018 | ≤ 4.17 | $1.81^{+0.15}_{-0.14}$ | $6.45^{+0.78}_{-0.78}$ | 64.2(75) |
| SDSS 0231-0728 | ≤ 19.90 | $1.85^{+0.33}_{-0.31}$ | $2.10^{+0.59}_{-0.58}$ | 25.3(43) |
| PSS 0926+3055 | ≤ 1.02 | $1.99^{+0.08}_{-0.08}$ | $17.58^{+1.15}_{-1.15}$ | 76.1(78) |
| PSS 1326+0743 | ≤ 0.47 | $1.87^{+0.10}_{-0.10}$ | $12.54^{+0.84}_{-1.13}$ | 51.2(65) |
| Q 0000-263 | ≤ 0.40 | $2.02^{+0.07}_{-0.07}$ | $12.59^{+0.75}_{-0.75}$ | 71.3(82) |
| BR 0351-1034 | ≤ 5.29 | $1.76^{+0.31}_{-0.26}$ | $5.24^{+0.96}_{-0.97}$ | 8.7(10) |
| SDSS 1030+0524 | ≤ 7.77 | $1.92^{+0.23}_{-0.21}$ | $1.39^{+0.23}_{-0.23}$ | 40.9(44) |
| BR 2237-0607 | ≤ 3.30 | $2.09^{+0.22}_{-0.21}$ | $3.82^{+0.59}_{-0.57}$ | 20.4(25) |

NOTE. — The best-fit photon index, normalization, and χ^2 were obtained from a model consisting of a Galactic-absorbed power-law without any intrinsic absorption.

^aIntrinsic column density in units of 10^{22} cm^{-2} . Upper limits were calculated using the intrinsically-absorbed power-law model with Galactic absorption, and represent 90% confidence limits for each value, taking one parameter of interest ($\Delta\chi^2=2.71$; e.g., Avni 1976).

^bPower-law normalization for the pn data, taken from joint fitting of all three EPIC detectors with the Galactic-absorbed power-law model; units are $10^{-6} \text{ keV cm}^{-2} \text{ s}^{-1} \text{ keV}^{-1}$.

events with $\text{FLAG}=0$, and $\text{PATTERN} \leq 12$ ($\text{PATTERN} \leq 4$) and $200 \leq \text{PI} \leq 12000$ ($150 \leq \text{PI} \leq 15000$) for the MOS (pn) detectors. The event files of the observations of SDSS 0210-0018, SDSS 0231-0728, and PSS 0926+3055 were also filtered to remove periods of flaring activity, which were apparent in the light curve of the entire full-frame window. Such flaring activity, which originates in the Earth's magnetosphere, depends on several unpredictable factors, and it can significantly reduce the good-time intervals of an observation.⁸ The observations of SDSS 0210-0018, SDSS 0231-0728, and PSS 0926+3055 were shortened by 16 ks, 10 ks, and 0.6 ks, respectively, as a result of this filtering. The event files of the PSS 0121+0347 and PSS 1326+0743 observations were not filtered in time, since the entire observation of the first source was performed during a moderate background flare period with count rates ~ 3 times higher than nominal values, and the full-frame count-rate light curve of the second source did not show any flaring. The exposure times listed in Table 1 reflect the filtered data used in the analysis.

We searched for X-ray emission from an additional radio-quiet AGN, SDSS J021102.72-000910.3 at $z=4.90$ (Fan et al. 1999), which lies close to the edge of the field of view in the *XMM-Newton* observation of SDSS 0210-0018. The former source is not detected, and the 3σ detection thresh-

⁸ On average, $\sim 35\%$ of the data from *XMM-Newton* observations with exposure times greater than 10 ks are lost due to flaring (K. Kuntz, 2005, private communication). For more details see the *XMM-Newton* User Handbook at http://xmm.vilspa.esa.es/external/xmm_user_support/documentation/uhb/index.html

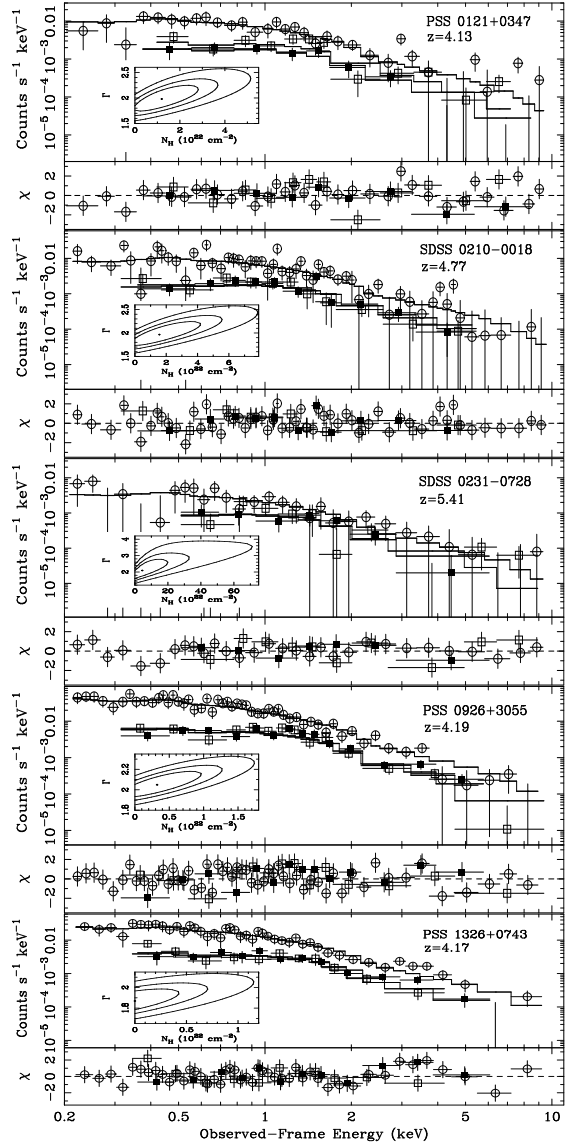


FIG. 1.— Data, best-fit spectra, and residuals for our new *XMM-Newton* observations of five $z > 4$ AGNs. Open circles, filled squares, and open squares represent the pn, MOS1, and MOS2 data, respectively. Solid lines represent the best-fit model for each spectrum, and the thick line marks the best-fit model for the pn data. The χ residuals are in units of σ with error bars of size one. The inset in each panel shows 68, 90, and 99% confidence contours for the intrinsic absorption (N_{H}) and photon index (Γ).

old is ~ 120 counts. Using PIMMS,⁹ this translates to an upper limit on the unabsorbed observed-frame 0.5–2 keV flux of $\lesssim 10^{-14} \text{ ergs cm}^{-2} \text{ s}^{-1}$, which is consistent with the $3.1^{+2.2}_{-1.4} \times 10^{-15} \text{ ergs cm}^{-2} \text{ s}^{-1}$ flux measured by Vignali et al. (2001).

2.2. Spectral Analysis

To extract X-ray spectra we used a source-extraction aperture radius of $30''$ in the images of all three European Photon Imaging Camera (EPIC) detectors for all but one AGN, PSS 0121+0347. For this source we used an aperture radius of $20''$ for the source extraction, since a larger aperture was affected by the (mainly hard X-ray) background flare, resulting in a hardening of the spectrum and a lowering of the signal-

⁹ Portable Interactive Multi-Mission Simulator at <http://heasarc.gsfc.nasa.gov/Tools/w3pimms.html>

TABLE 3
FLUXES, LUMINOSITIES, AND α_{ox} FOR THE SAMPLE OF $z > 4$ AGNs

| AGN | $\text{AB}_{1450(1+z)} \text{\AA}$ | M_B | $f_V[2500(1+z) \text{\AA}]^a$ (mJy) | $\log vL_V(2500 \text{\AA})$ (ergs s $^{-1}$) | Optical Ref. | $F_{0.5-2 \text{ keV}}^b$ | $\log L_{2-10 \text{ keV}}$ (ergs s $^{-1}$) | α_{ox} |
|----------------|------------------------------------|-------|--|---|-----------------|---------------------------|--|-------------------------|
| PSS 0121+0347 | 18.5 | -28.3 | 0.222 ± 0.071 | 46.94 | 1 | $17.02_{-2.28}^{+2.19}$ | 45.51 | $-1.65_{-0.03}^{+0.03}$ |
| SDSS 0210-0018 | 19.3 | -27.7 | 0.106 ± 0.011 | 46.71 | 2 | $14.37_{-1.76}^{+1.77}$ | 45.27 | $-1.54_{-0.02}^{+0.03}$ |
| SDSS 0231-0728 | 19.3 | -27.9 | 0.062 ± 0.030 | 46.56 | 3 | $4.68_{-1.29}^{+1.35}$ | 45.21 | $-1.62_{-0.06}^{+0.06}$ |
| PSS 0926+3055 | 16.7 | -30.1 | 1.167 ± 0.042 | 47.67 | 1 | $39.04_{-2.54}^{+2.57}$ | 45.89 | $-1.76_{-0.01}^{+0.03}$ |
| PSS 1326+0743 | 17.2 | -29.6 | 0.736 ± 0.051 | 47.46 | 1 | $27.89_{-2.52}^{+1.90}$ | 45.73 | $-1.76_{-0.02}^{+0.03}$ |
| Q 0000-263 | 17.5 | -29.3 | 0.579 ± 0.058 | 47.35 | 4 | $12.59_{-0.75}^{+0.75}$ | 45.72 | $-1.70_{-0.01}^{+0.03}$ |
| BR 0351-1034 | 18.7 ^c | -28.2 | 0.185 ± 0.019 | 46.89 | 5 | $11.69_{-2.19}^{+2.22}$ | 45.39 | $-1.69_{-0.04}^{+0.04}$ |
| SDSS 1030+0524 | 19.7 | -27.8 | 0.076 ± 0.008 | 46.75 | 6 | $3.09_{-0.52}^{+0.53}$ | 45.18 | $-1.69_{-0.04}^{+0.04}$ |
| BR 2237-0607 | 18.3 ^c | -28.5 | 0.267 ± 0.027 | 47.08 | 5 | $8.50_{-1.27}^{+1.34}$ | 45.32 | $-1.74_{-0.03}^{+0.04}$ |
| SDSS 1306+0356 | 19.6 | -27.9 | 0.085 ± 0.008 | 46.76 | 6 | $2.74_{-0.53}^{+0.56}$ | 45.07 | $-1.75_{-0.05}^{+0.05}$ |

REFERENCES. — (1) Vignali et al. (2003a); (2) Vignali et al. (2001); (3) Vignali et al. (2003b); (4) Schneider, Schmidt, & Gunn (1989); (5) Storrie-Lombardi et al. (1996); (6) Brandt et al. (2002)

^a Assuming an ultraviolet (UV) continuum of the form: $f_V \propto v^{-0.79}$ (Fan et al. 2001).

^b Galactic absorption-corrected flux in the observed 0.5–2 keV band in units of 10^{-15} ergs cm $^{-2}$ s $^{-1}$.

^c Estimated using an empirical relation between the APM R and $\text{AB}_{1450(1+z)} \text{\AA}$ magnitudes and redshift; see § 2 of Kaspi et al. (2000).

to-noise ratio. For a nominal background level, increasing the aperture radius from $20''$ to $30''$ should not have resulted in any noticeable change in either photon index or normalization (Kirsch et al. 2004). Background regions were taken to be at least as large as the source regions; these were annuli, when there were no neighboring sources, and circles otherwise. The redistribution matrix files (RMFs; which include information on the detector gain and energy resolution) and the ancillary response files (ARFs; which include information on the effective area of the instrument, filter transmission, detector window transmission and efficiency, and any additional energy dependent effects) for the spectra were created with the SAS tasks RMFGEN and ARFGEN, respectively.¹⁰ We note that the two reflection grating spectrometer detectors on *XMM-Newton* do not have sufficient counts to perform a high-resolution spectral analysis for any of our sources.

The spectra were grouped with a minimum of 10–25 photons per bin using the task GRPPHA. For each AGN we used XSPEC v11.3.0 (Arnaud 1996) to fit the data with the following models: (i) a power-law model and a Galactic absorption component (Dickey & Lockman 1990), which was kept fixed during the fit, and (ii) a model similar to the first with an added intrinsic (redshifted) neutral absorption component. In all the fits we assumed solar abundances (Anders & Grevesse 1989) and used the PHABS absorption model in XSPEC with the Balucinska-Church & McCammon (1992) cross-sections. We fitted the data from each EPIC detector alone, jointly fitted the data of the two MOS detectors, and jointly fitted all three EPIC detectors with these models. In general, the five

different fitting results were consistent with each other within the uncertainties, and the joint fit of all three EPIC detectors had the smallest uncertainty on the spectral parameters. The best-fit results for the joint fit of the three EPIC detectors are summarized in Table 2 (first five sources). For all five sources the best-fit model is a Galactic-absorbed power law; an F -test carried out on the data does not warrant the addition of an intrinsic absorber in any of the spectra. The 90% confidence upper limits on intrinsic N_{H} appear in Table 2. The spectra of the five AGNs and their best-fit models appear in Fig. 1. Also shown for each AGN is a confidence-contour plot of the Γ – N_{H} parameter space. No strong systematic residuals are seen for any of the fits. Optical fluxes and luminosities, and X-ray fluxes and luminosities of the sources computed using the best-fit spectral parameters of Table 2, appear in Table 3 (first five sources).

2.3. Serendipitous Sources

Since the luminous AGNs under study are probably associated with massive potential wells in the earliest collapsed large-scale structures, we searched for candidate $z > 4$ AGNs in the *XMM-Newton* images of three of our sources with SDSS imaging (SDSS 0210-0018, SDSS 0231-0728, and PSS 1326+0743) to search for AGN clustering on scales of ≈ 0.1 –5 Mpc at $z \sim 4$ –5 (e.g., see Djorgovski et al. 2003; Vignali et al. 2003b; Hennawi et al. 2005). We matched X-ray and SDSS sources in those fields and utilized the Richards et al. (2002) color criteria as well as a pointlike morphology criterion to identify ≈ 3 X-ray emitting $z \gtrsim 4$ AGN candidates for future optical spectroscopy.

¹⁰ For more details see the NASA/GSFC calibration memo CAL/GEN/92-002 at http://heasarc.gsfc.nasa.gov/docs/heasarc/caldb/docs/memos/cal_gen_92_002/cal_gen_92_002.html

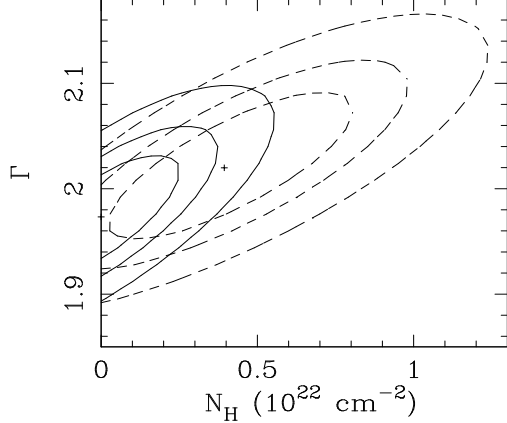


FIG. 2.— 68, 90, and 99% confidence regions for the photon index vs. intrinsic column density derived from joint spectral fitting of our sample of eight radio-quiet AGNs. Solid (dashed) contours refer to the entire (common) energy range of the AGNs (see § 4 for more details).

3. ARCHIVAL SAMPLE OF $Z > 4$ RADIO-QUIET AGNS

To improve the statistics on X-ray spectral properties, we expanded the sample by adding moderate-to-high quality data of five radio-quiet $z > 4$ AGNs, obtained from the *XMM-Newton* and *Chandra* archives. A minimum of ~ 200 (~ 100) photons per source from *XMM-Newton* (*Chandra*) observations was considered useful to our analysis. The observation log of the four sources observed by *XMM-Newton* appears in Table 1, which also gives the references to the original papers presenting the results of those observations. We processed the observation data files of these sources following the analysis procedures described in § 2. As in the case of our original sample, we were only able to place upper limits upon the intrinsic column densities in these sources. The best-fit model parameters for the X-ray spectra of these sources are listed in Table 2.

The fifth observation, a 118 ks *Chandra*/ACIS-S observation of SDSS J130608.26+035626.3 (hereafter SDSS 1306+0356) at $z=5.99$ in 2003 November 29–30, was re-analyzed following the same source and background extraction parameters as those used in the original paper reporting that observation (Schwartz & Virani 2004) applying standard CIAO¹¹ v3.2 routines to the data. The events were grouped into bins that had a minimum of 15 counts per bin, and the model fit to the data included a constant Galactic absorption component ($N_{\text{H}}=2.07 \times 10^{20} \text{ cm}^{-2}$), a power-law component, and a neutral Fe K α line at rest-frame 6.4 keV with a width of $\sigma=0.1$ keV, since there is a feature in the spectrum at that location hinting at the presence of such a line (see Schwartz & Virani 2004). The best-fit photon index is $\Gamma=1.82_{-0.31}^{+0.29}$, the flux normalization at 1 keV is $(1.23 \pm 0.24) \times 10^{-6} \text{ keV cm}^{-2} \text{ s}^{-1} \text{ keV}^{-1}$, and the Fe K α rest-frame equivalent width is $1.0_{-0.8}^{+1.1} \text{ keV}$.

The optical fluxes and luminosities, and X-ray fluxes and luminosities of the five sources, based upon the best-fit spectral parameters of Table 2 and of the single *Chandra* observation, are listed in Table 3. Plots of the spectra and best-fit models, which are generally consistent with our results, appear in the original papers cited in Table 1 and in Schwartz & Virani (2004) for the single *Chandra* observation.

4. JOINT SPECTRAL FITTING OF $Z > 4$ RADIO-QUIET AGNS

To derive the best possible constraints on the average X-ray spectral properties of radio-quiet $z > 4$ AGNs, we jointly fitted the spectra of the expanded sample of eight radio-quiet AGNs (e.g., see § 6 of Vignali et al. 2005). We combined the spectra from all the detectors of the observations of the eight AGNs, 22 datasets in total, and used XSPEC to fit their spectra jointly. We fit two different models: (i) a power-law that includes both Galactic and intrinsic absorption, and (ii) a power-law with Galactic absorption including a Compton-reflection component, using the PEXRAV model in XSPEC (Magdziarz & Zdziarski 1995), and a neutral narrow Gaussian Fe K α line. The Compton-reflection component, also known as a Compton-reflection ‘hump’, is the spectral manifestation of hard X-ray photons emitted in a corona of hot electrons and reflected off the relatively colder accretion disk (e.g., see § 3.5 of Reynolds & Nowak 2003 and references therein). The Compton-reflection hump feature is observed in the rest-frame ~ 7 –60 keV energy range, peaking at rest-frame ~ 30 keV. The joint-fitting process was carried out twice for both models; first, to include the entire energy range of all the datasets, and a second time to include only the common rest-frame energy range of the eight sources: $1.5 \lesssim E_{\text{rest}} \lesssim 51$ keV. The total number of photons used in the joint-fitting process is ~ 7000 (~ 6400 for the common energy range), and it is larger by an order of magnitude than the number of counts used in the joint fitting of 48 $z > 4$ radio-quiet AGNs by Vignali et al. (2005).

The fitting process with the first model required that all datasets be fitted with a single power-law and a single intrinsic absorption column. Therefore the photon index and intrinsic absorption column were each tied to a single value across all data sets, and these two parameters were allowed to vary jointly (see the discussion of intrinsic dispersion in § 5.1 as partial justification of this approach). The power-law normalizations of all data sets were allowed to vary freely. For the second model we used a single power-law and a single relative-reflection component (R , where R is defined as $\Omega/2\pi$ and Ω is the solid angle subtended by the reflecting medium) of the Compton hump for all datasets, and allowed them to vary jointly. We fixed the rest-frame energy and width (σ) of the neutral Fe K α line to 6.4 and 0.1 keV, respectively, and tied all the power-law and Gaussian normalizations to two different values, allowing them to vary jointly; each dataset was assigned a constant scaling factor to account for the different flux levels of each AGN and each detector. The best-fit values and upper limits for the parameters used in the joint fits are given in Table 4. Fig. 2 is a contour plot of Γ versus N_{H} as a result of the joint-fitting process using the first model. The noticeable difference between the confidence contours in the entire and common energy ranges stems from the fact that the two AGNs at $z \simeq 6$ increase the low-energy threshold in the common energy range, and as a consequence many low-energy photons from the X-ray bright AGNs at $z \simeq 4.2$ are ignored in the fit. This causes the upper limit on the intrinsic absorption in the common energy range to rise significantly relative to the upper limit when using the entire energy range.

We repeated the joint-fitting process with the first model and fitted the four most optically luminous radio-quiet sources separately from the four least optically luminous radio-quiet sources both for the entire and common energy ranges of the two sub-samples. Both Γ and N_{H} in the two luminosity

¹¹ *Chandra* Interactive Analysis of Observations. See <http://asc.harvard.edu/ciao/>

TABLE 4
BEST-FIT PARAMETERS FROM JOINT FITTING OF EIGHT RADIO-QUIET $z > 4$ AGNS

| Spectral Model Galactic-Absorbed Power Law and | Energy Range ^a | N_{H} (10^{22} cm^{-2}) | Γ | EW(Fe K α) ^b (eV) | R^c | $\chi^2(\text{DOF})$ |
|---|------------------------------|---|------------------------|---|-------------|----------------------|
| Intrinsic Absorption | E | ≤ 0.28 | $1.97^{+0.06}_{-0.04}$ | ... | ... | 308.3 (360) |
| Intrinsic Absorption | C | ≤ 0.84 | $2.02^{+0.04}_{-0.06}$ | ... | ... | 291.3 (338) |
| Compton-Reflection and neutral Fe K α line | E | ... | $1.98^{+0.10}_{-0.09}$ | ≤ 189 | ≤ 1.22 | 306.0 (359) |
| Compton-Reflection and neutral Fe K α line | C | ... | $1.95^{+0.10}_{-0.08}$ | ≤ 191 | ≤ 1.03 | 291.2 (337) |

^aE - entire energy range of all the spectra. C - the common rest-frame energy range among all sources (1.5–51 keV).

^bRest-frame equivalent width calculated with a mean redshift of 4.8.

^cCompton hump relative reflection parameter (see Magdziarz & Zdziarski 1995).

groups are consistent with one another and with the values we obtain by fitting the entire radio-quiet sample. For the fitting using the entire energy range, we measure $\Gamma=1.99\pm 0.06$ for the most-luminous sources and $\Gamma=1.95^{+0.23}_{-0.20}$ for the least-luminous sources.

5. RESULTS AND DISCUSSION

5.1. X-ray Photon Index

The photon indices and their uncertainties for the full sample of ten AGNs, in the ~ 1 –50 keV rest-frame energy range (the range where most photons are detected), are listed in Table 2. A statistical summary of our expanded sample’s photon-index distribution appears in Table 5. Using the maximum likelihood method of Maccacaro et al. (1988) we find no significant intrinsic dispersion in Γ ; this is expected since the individual uncertainties on Γ are larger than the spread in individual Γ values. In Fig. 3 we plot Γ versus absolute B magnitude and redshift for our expanded sample, together with previous measurements of the photon index in other AGN samples (see § 6 of Vignali et al. 2005 and references therein). There is no obvious systematic difference between the photon indices of our radio-quiet sources and those of luminous AGNs observed at lower redshifts (e.g., the Piconcelli et al. 2005 sample of nearby AGNs). Using a Spearman rank correlation method we find no significant correlations between Γ in radio-quiet sources and either luminosity or redshift as also found at lower redshift ($z \lesssim 0.4$) by, e.g., Porquet et al. (2004). Applying a linear regression algorithm that accounts for intrinsic scatter and measurement errors (Akritas & Bershady 1996), we obtain $|\partial\Gamma/\partial z| < 0.04$ for the 51 radio-quiet AGNs plotted in Fig. 3. From the joint fitting of eight radio-quiet AGN spectra using the absorbed power-law model we find $\Gamma = 1.97^{+0.06}_{-0.04}$. This is consistent with both the unweighted mean of the individual Γ values and the counts-weighted mean Γ for the radio-quiet sample.

The mean photon indices we find for $z > 4$ radio-quiet AGNs are also all consistent with those calculated by Vignali et al. (2005). All these photon-index values confirm and strengthen the Vignali et al. (2005) result that the X-ray photon index does not depend on optical luminosity or redshift. In particular, our results do not support either of the reports for a significantly different photon index at low versus high redshift (Bechtold et al. 2003; Grupe et al. 2005). Bechtold et al. (2003) used a heterogeneous sample of low-redshift ROSAT sources and high-redshift sources detected with *Chandra*. The

mix of different datasets may have produced a bias which led Bechtold et al. (2003) to report a flattening of Γ at higher redshift (e.g., due to spectral curvature at low energies and mission-to-mission cross-calibration uncertainties). In addition, the counts-weighted mean Γ of their $z > 4$ *Chandra* sources is 1.50 ± 0.15 (see their Table 2). This is significantly lower than the average Γ of $1.93^{+0.10}_{-0.09}$ for 48 radio-quiet AGNs, including the Bechtold et al. (2003) sources, obtained by Vignali et al. (2005). Comparing the photon indices of our four sources which overlap with those of Grupe et al. (2005) shows that in three cases the values are in good agreement. However, for SDSS 1030+0524 the $\Gamma=2.65\pm 0.34$ found by Grupe et al. (2005) is significantly steeper, and is inconsistent both with the value we obtain, $\Gamma=1.92^{+0.22}_{-0.21}$, and that obtained by Farrah et al. (2004), $\Gamma=2.12\pm 0.11$. The photon index we obtain for SDSS 1030+0524, while slightly harder, is compatible within the errors with the one found by Farrah et al. (2004). By inspection of Tables 1 and 4 of Grupe et al. (2005) it is also apparent that the relatively steep mean Γ they report for their radio-quiet sources, 2.23 ± 0.48 , is an unweighted mean dominated by sources with limited photon statistics (≈ 50 counts), which in most cases result in best-fit Γ exceeding a value of 2.2.

The insignificant dispersion in individual Γ values for our $z > 4$ AGN sample may partially be driven by a selection bias, since we specifically targeted some of the most X-ray luminous AGNs known. However, observing down the AGN luminosity function at $z > 4$ is challenging with existing X-ray observatories. In fact, the faintest X-ray sources at those redshifts with enough counts to allow meaningful measurement of the photon index were detected in the 2 Ms *Chandra* Deep Field North survey (Vignali et al. 2002; see Table 1 of Brandt et al. 2005 for a list of X-ray faint AGNs at $z > 4$). The best studied source in that survey, CXO HDFN J123647.9+620941 at $z=5.19$ and with $L_{2-10 \text{ keV}}=10^{44.0} \text{ ergs s}^{-1}$, has $\Gamma=1.8\pm 0.3$, which is consistent with the photon indices we find for our sources (Vignali et al. 2002). The photon indices of our least luminous sources do not appear to be significantly different from those of the more luminous ones both individually and on average by splitting the joint spectral fit into two luminosity groups (see § 4). Inspection of Table 4 of Vignali et al. (2005) also does not show a strong dependence of Γ on optical luminosity. In spite of being extremely luminous, our $z > 4$ AGNs are otherwise representative of the AGN population by having ‘normal’ rest-frame UV properties (i.e., no broad ab-

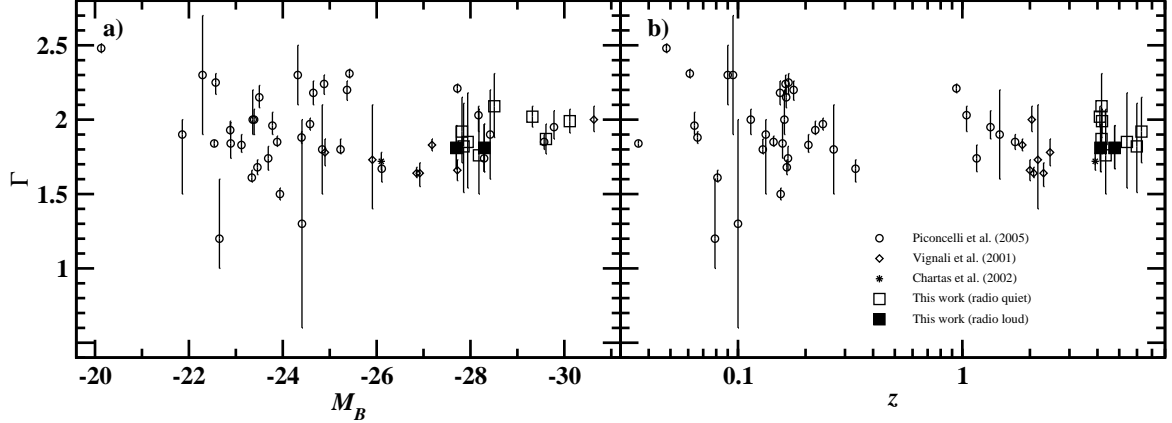


FIG. 3.— The X-ray photon index (Γ), versus (a) absolute B magnitude and (b) redshift, adapted from Vignali et al. (2005). The eight (two) radio-quiet (moderately radio-loud) AGNs presented in this work are marked with open (filled) squares. Note that the photon index does not show any clear dependence on either luminosity or redshift.

TABLE 5
PHOTON INDEX STATISTICS OF $z > 4$ AGNS

| Statistic | Entire Sample | Photon Index (Γ) Radio-Quiet Sources |
|-------------------------------|---------------|--|
| Unweighted Mean | 1.89 | 1.92 |
| Unweighted Standard Deviation | 0.11 | 0.11 |
| Unweighted Error of the Mean | 0.03 | 0.04 |
| Counts-Weighted Mean | 1.93 | 1.95 |
| Median | 1.86 | 1.90 |

sorption lines, typical emission-line properties and rest-frame UV continua; Vignali et al. 2001, 2003a, b). Recent multi-wavelength observations of $z > 4$ AGNs have found that their overall spectral energy distributions (SEDs) are not significantly different from those of lower redshift sources implying no SED evolution (e.g., see Carilli et al. 2001 and Petric et al. 2003 for radio observations; Pentericci et al. 2003 and Vanden Berk et al. 2001 for UV-optical observations). We argue that the broad-band X-ray spectral properties of $z > 4$ AGNs are also not significantly different than those of lower redshift sources.

5.2. Intrinsic Absorption

In all the individual fits of the $z > 4$ AGNs we obtained an intrinsic N_{H} consistent with zero with 90% confidence. Table 2 lists the upper limits on the intrinsic absorption; they are all in the range $\approx 10^{22}\text{--}10^{23} \text{ cm}^{-2}$. The joint-fitting procedure yielded an upper limit on the common intrinsic N_{H} of $\sim (3\text{--}8) \times 10^{21} \text{ cm}^{-2}$ (Table 4 and Fig. 2). These constraints on intrinsic absorption are the tightest presented to date for $z > 4$ AGNs, and our individual-fitting results are less prone to bias than the joint-fitting results that have been predominantly utilized previously.¹² Our results show that radio-quiet AGNs at $z > 4$ do not appear to have higher absorption columns than their lower redshift counterparts. The metallicity in the inner regions of high-redshift AGNs may be higher, on average, than in their lower-redshift counterparts

¹² Since photoelectric absorption by neutral gas is an extremely strong spectral effect, a column density derived via joint fitting of several sources may not always be a good estimate of their ‘typical’ column density. The presence of even one source with significant low-energy flux can bias the joint-fitting column density downward, since such flux is highly inconsistent with a strong photoelectric-absorption cutoff at low energy.

mainly due to their higher luminosities (e.g., Dietrich et al. 2003). Since X-ray photoelectric absorption is predominantly due to metals and not hydrogen, the inferred intrinsic neutral hydrogen column density depends upon the assumed metallicity. Therefore, N_{H} values are inversely proportional to the assumed metallicity, and the quoted upper limits on the best-fit intrinsic columns given in Table 4 are conservative values (as solar abundances were assumed).

Despite the considerable large-scale evolution the Universe has experienced since $z \approx 6$, and in particular the strong evolution in the AGN population (e.g., Fan et al. 2003; Croom et al. 2004; Barger et al. 2005; Brandt & Hasinger 2005), we do not detect significant changes in the central regions of luminous radio-quiet AGNs. Since the host galaxies of AGNs at high redshifts are probably still in the formation process, one might expect large amounts of gas and dust in the interstellar medium of these hosts that could increase the amount of line-of-sight absorption. Signatures of large amounts of interstellar molecular gas and dust have been recently detected in some of the most distant AGNs (e.g., Carilli et al. 2001; Bertoldi et al. 2003; Walter et al. 2003; Maiolino et al. 2004). In addition, the fact that radio-loud AGNs show signs for increased intrinsic absorption with redshift (see § 1), makes it of interest to check if there is a similar trend for the radio-quiet population. Our results do not show significant intrinsic absorption in any of the $z > 4$ radio-quiet AGNs, which is in broad agreement with, e.g., the Laor et al. (1997) results for local radio-quiet AGNs. We caution that our AGN sample is far from being complete or representative of the entire AGN population. We have specifically considered only optically and X-ray bright, radio-quiet AGNs with no broad absorption lines. Steffen et al. (2003) have found that the fraction of type 1 (i.e., unobscured) AGNs increases with X-ray luminosity, suggesting luminosity-dependent absorption. It is therefore possible that the relatively lower intrinsic absorption in our sources is a consequence of them being among the most luminous AGNs known.

5.3. $\text{Fe K}\alpha$ Line and Compton Reflection

The joint-fitting process placed respectable constraints on the strength of a putative neutral narrow $\text{Fe K}\alpha$ line; a 90% confidence upper limit on the rest-frame equivalent width is $\sim 190 \text{ eV}$. We also constrained the relative reflection component of a Compton-reflection hump (see Table 4). These are the best constraints to date on these properties

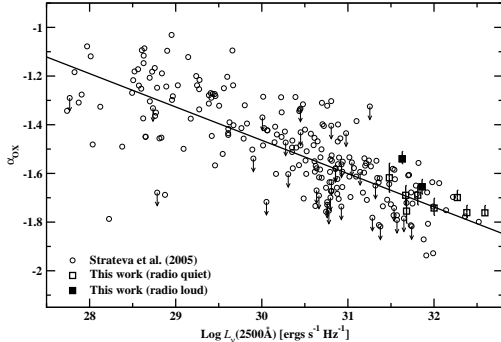


FIG. 4.— The optical-to-X-ray SED parameter, α_{ox} , versus luminosity density at 2500 Å. The ten AGNs studied in this work (squares) follow the Strateva et al. (2005) $\alpha_{\text{ox}}-L_{\nu}(2500 \text{ \AA})$ relation (solid line), $\alpha_{\text{ox}} = -0.136 \times L_{\nu}(2500 \text{ \AA}) + 2.616$. The two moderately radio-loud sources presented in this work, PSS 0121+0347 and SDSS 0210-0018, are the only such sources on this diagram and are marked with filled squares. The reason why most of our sources lie above the best-fit line may be attributed to the fact that we specifically targeted X-ray bright sources.

of $z > 4$ AGNs. Due to the high mean X-ray luminosity ($\langle \log L_{2-10 \text{ keV}}(\text{ergs s}^{-1}) \rangle \simeq 45.5$) of our sample, both the Fe K α line and Compton hump are expected to be relatively weak. Using the recent Page et al. (2004a) anticorrelation between EW(Fe K α) and $L_{2-10 \text{ keV}}$ (the so-called Fe K α “Baldwin Relation”), we find an empirically expected range of $\text{EW}(\text{Fe K}\alpha) \sim 25-80 \text{ eV}$ for our sources, several times lower than our upper limit (but see also Jimenez-Bailón et al. 2005). Given our results, the $\text{EW}(\text{Fe K}\alpha) \approx 1 \text{ keV}$ for SDSS 1306+0356 (see § 3) appears remarkable and should be investigated with better data. The constraints we obtain on the Compton-reflection component, $R \lesssim 1.2$, are consistent with those obtained for some $z \approx 0-1$ AGNs (e.g., Page et al. 2004b), but are significantly lower than the value $R=2.87 \pm 0.96$ found in PG 1247+267 at $z=2.04$, the most luminous source in which such a component was significantly detected (Page et al. 2004b).

5.4. Optical-to-X-ray SED

For each of the ten AGNs we computed the optical-to-X-ray SED parameter, α_{ox} , defined as:

$$\alpha_{\text{ox}} = \frac{\log(f_{2 \text{ keV}}/f_{2500 \text{ \AA}})}{\log(v_{2 \text{ keV}}/v_{2500 \text{ \AA}})} \quad (1)$$

where $f_{2 \text{ keV}}$ and $f_{2500 \text{ \AA}}$ are the flux densities at rest-frame 2 keV and 2500 Å, respectively (e.g., Tananbaum et al. 1979).

The α_{ox} values and their 1σ errors appear in Table 3. The errors on α_{ox} were computed following the “numerical method” described in § 1.7.3 of Lyons (1991), taking into account the uncertainties on the X-ray power-law normalizations and photon indices, and the effects of possible changes in the UV-optical slope (from $\alpha=-0.5$ to -0.79). In Fig. 4 we plot α_{ox} for our sources against their optical luminosities, and include a sample of 228 radio-quiet AGNs (mainly from the SDSS) from Strateva et al. (2005) in the diagram. Also plotted in Fig. 4 is the best-fit line of the Strateva et al. (2005) $\alpha_{\text{ox}}-L_{\nu}(2500 \text{ \AA})$ relation (Eq. 6 of Strateva et al. 2005). The α_{ox} values of the ten AGNs presented in this work, which represent extreme luminosities and redshifts, generally follow that relation, although most of them lie above the best-fit line. This may be due to a selection bias since we have specifically targeted X-ray bright sources.

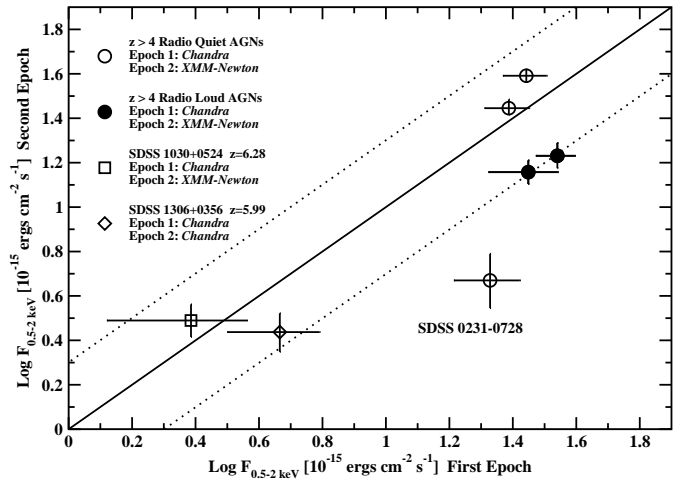


FIG. 5.— Two-epoch Galactic-absorption corrected 0.5–2 keV fluxes for seven of the $z > 4$ AGNs in our sample. The solid line marks the 1:1 flux ratio, and the two dotted lines mark 1:2, and 2:1 flux ratios, to guide the eye. SDSS 0231-0728 clearly varied by more than a factor of two between the two epochs. The second and third most variable sources, PSS 0121+0347 and SDSS 0210-0018, are moderately radio loud and are marked with filled circles.

5.5. X-ray Variability

Using the event files of our *XMM-Newton* observations, we searched for rapid (~ 1 hr timescale in the rest frame) variability of the AGNs by applying Kolmogorov-Smirnov tests to the lists of photon arrival times. No significant variations were detected, and the fractional variability of the count-rate light curves was smaller than 15% in all cases. To test if the X-ray flux exhibits long-term (months-to-years) variations in our sample, we list in Table 6 pairs of two-epoch 0.5–2 keV fluxes for seven $z > 4$ sources which were observed with *Chandra* in the first epoch, and with either *XMM-Newton* or *Chandra* in the second epoch. The relative uncertainties between flux measurements obtained with *XMM-Newton* versus those obtained with *Chandra* are considered to be the smallest among different X-ray observatories, and are normally $\lesssim 10\%$ (Snowden 2002; S. Snowden, 2005, private communication). Table 6 also lists the rest-frame temporal separation between the two observations, and a χ^2 statistic to quantify the significance of variation between the two epochs. The null hypothesis is that the flux in each epoch is equal to the mean flux of the two epochs. A larger χ^2 implies higher significance of variability, and values larger than 2.71 (6.63) imply that the two fluxes are inconsistent within their uncertainties, i.e., there is significant variability at a 90% (99%) confidence level (e.g., Avni 1976). Of the seven AGNs studied only two sources, PSS 1326+0743 and SDSS 1030+0524, do not show a significant (i.e., at $\geq 90\%$ confidence) long-term variation. Fig. 5 plots the fluxes of the second epoch against those of the first, as given in Table 6.

While most AGNs varied by no more than a factor of ≈ 2 between the two epochs one source, SDSS 0231-0728, faded by a factor of ~ 4 between the first (*Chandra*) observation and the second (*XMM-Newton*) one. This flux change occurred over a rest-frame period of 73 d. This is the largest change in X-ray flux observed in a $z > 4$ radio-quiet AGN (e.g., Paoletti et al. 2004). Given the optical flux of the source, and using the Vignali et al. (2003b) relation between optical and X-ray fluxes, it is likely that this source was caught in an X-ray high state in the first epoch (Vignali et al. 2003b), since its X-ray flux in the second epoch (this work) agrees with

TABLE 6
TWO-EPOCH X-RAY FLUXES OBTAINED BY *XMM*-Newton AND *Chandra*

| AGN | First Epoch | | Second Epoch | | Δt^b (days) | χ^2^c |
|----------------|---|------|---|------|------------------------|------------|
| | $F_{0.5-2 \text{ keV}}^a$ ($10^{-15} \text{ ergs cm}^{-2} \text{ s}^{-1}$) | Ref. | $F_{0.5-2 \text{ keV}}^a$ ($10^{-15} \text{ ergs cm}^{-2} \text{ s}^{-1}$) | Ref. | | |
| PSS 0121+0347 | $34.7^{+5.4}_{-4.4}$ | 1 | $17.02^{+2.19}_{-2.28}$ | 2 | 135 | 20.40 |
| SDSS 0210-0018 | $28.1^{+8.1}_{-6.0}$ | 3 | $14.37^{+1.77}_{-1.76}$ | 2 | 258 | 16.35 |
| SDSS 0231-0728 | $21.3^{+5.6}_{-4.6}$ | 4 | $4.68^{+1.35}_{-1.29}$ | 2 | 73 | 41.42 |
| PSS 0926+3055 | $27.7^{+4.7}_{-4.1}$ | 1 | $39.04^{+2.57}_{-2.54}$ | 2 | 186 | 6.43 |
| PSS 1326+0743 | $24.4^{+4.3}_{-3.6}$ | 1 | $27.89^{+1.90}_{-2.52}$ | 2 | 139 | 0.64 |
| SDSS 1030+0524 | $2.43^{+1.48}_{-0.99}$ | 5 | $3.09^{+0.53}_{-0.52}$ | 6 | 68 | 0.45 |
| SDSS 1306+0356 | $4.63^{+1.77}_{-1.33}$ | 5 | $2.74^{+0.56}_{-0.53}$ | 7 | 96 | 3.35 |

REFERENCES. — (1) Vignali et al. (2003a); (2) This work; (3) Vignali et al. (2001); (4) Vignali et al. (2003b); (5) Brandt et al. (2002); (6) Farrah et al. (2004); (7) Schwartz & Virani (2004)

^aGalactic absorption-corrected flux in the observed 0.5–2 keV band. Errors represent 90% confidence limits on the fluxes.

^bRest-frame time difference between the two epochs.

^cVariability statistic; see § 5.5.

the value predicted from its optical flux (assuming the optical flux is nearly constant). Vignali et al. (2003b) also noted that SDSS 0231–0728 was X-ray brighter than expected (see their Fig. 5). The spectral slope of the source also shows a possible indication of flattening from $\Gamma=2.8^{+1.10}_{-0.95}$ to $\Gamma=1.85^{+0.33}_{-0.31}$ between the two epochs, but the significance is only $\sim 1\sigma$ due to the limited number of counts (~ 25) in the first *Chandra* snapshot observation. This is a tentative indication for a transition from a soft/high state to a hard/low state in this source, as has been seen for a few local AGNs (e.g., Guainazzi et al. 1998; Maccarone, Gallo, & Fender 2003).

6. SUMMARY AND FUTURE PROSPECTS

Moderate-to-high quality X-ray spectra of ten luminous AGNs at $z > 4$, including five new *XMM*-Newton observations, have been analyzed to extract X-ray spectral properties and search for flux variations. We found that the X-ray power-law photon index does not depend on either luminosity or redshift, broadly consistent with the lack of multiwavelength AGN SED evolution, and it has no detectable intrinsic dispersion at $z > 4$. Upper limits placed on the intrinsic absorption in eight radio-quiet $z > 4$ AGNs show that, on average, the X-ray light of luminous radio-quiet AGNs at $z > 4$ is not more absorbed than in nearby AGNs. All this suggests that the X-ray production mechanism and the central environment in radio-quiet AGNs do not depend on luminosity and have not evolved over cosmic time. We also place constraints on the strength of a putative narrow Fe K α line, and constrain the relative strength of the Compton-reflection hump at high rest-frame X-ray energies. Tighter constraints on those X-ray properties of luminous AGNs at $z > 4$, with existing X-ray observatories, can only be achieved by lengthy (several 100 ks) observations of the most luminous sources.

A search for short-timescale (~ 1 hr) X-ray variability found no significant variations, but on longer timescales (months-to-years) we have found significant variations in five of our sources, noting one extreme radio-quiet source in which the X-ray flux dropped by a factor of ~ 4 over a 73 d rest-frame

period; this is the most extreme X-ray variation ever observed for a radio-quiet AGN at $z > 4$. X-ray monitoring of SDSS 0231–0728 and other AGNs at high redshift will enable us to link the variability properties of high-redshift AGNs with some of their fundamental properties, such as BH mass, luminosity, and accretion rate, as is done at lower redshift (e.g., O’Neill et al. 2005). Two recent studies have reported that the X-ray flux variations of high-redshift AGNs are larger than those of their nearby counterparts (Manners et al. 2002; Paolillo et al. 2004). The data presented in this paper do not allow us to test this claim. Multiple-epoch X-ray observations of a large sample of high-redshift radio-quiet AGNs are required to investigate their variability properties, and compare them with those of the local AGN population.

This work is based on observations obtained with *XMM*-Newton, an ESA science mission with instruments and contributions directly funded by ESA Member States and the USA (NASA). We are grateful to Bret Lehmer and Divas Sanwal for help with the *XMM*-Newton data reduction. We also thank Aaron Steffen, Iskra Strateva, and Dan Vanden Berk for useful discussions. An anonymous referee is gratefully acknowledged for helping to improve the presentation of this paper. We gratefully acknowledge the financial support of NASA grant NNG04GF57G (OS, WNB, DPS), NASA LTSA grant NAG5-13035 (WNB, DPS), and NSF grants AST-0307582 (DPS), AST-0307409 (MAS), and AST-0307384 (XF). XF acknowledges support from an Alfred P. Sloan Research Fellowship, and a David and Lucile Packard Fellow in Science and Engineering. CV acknowledges support from MIUR cofin grant 03-02023 and INAF/PRIN grant 270/2003.

REFERENCES

Akritas, M. G., & Bershady, M. A. 1996, *ApJ*, 470, 706

Anders, E., & Grevesse, N. 1989, *Geochim. Cosmochim. Acta*, 53, 197

Anderson, S. F., et al. 2001, *AJ*, 122, 503

Arnaud, K. A. 1996, *ASP Conf. Ser.* 101: *Astronomical Data Analysis Software and Systems V*, 101, 17

Avni, Y. 1976, *ApJ*, 210, 642

Balucinska-Church, M., & McCammon, D. 1992, *ApJ*, 400, 699

Bechtold, J., et al. 2003, *ApJ*, 588, 119

Bertoldi, F., Carilli, C. L., Cox, P., Fan, X., Strauss, M. A., Beelen, A., Omont, A., & Zylka, R. 2003, *A&A*, 406, L55

Brandt, W. N., et al. 2002, *ApJ*, 569, L5

Brandt, W. N., et al. 2004, *Advances in Space Research*, 34, 2478

Brandt, W. N., & Hasinger, G. 2005, *ARA&A*, in press (astro-ph/0501058)

Cappi, M., Matsuoka, M., Comastri, A., Brinkmann, W., Elvis, M., Palumbo, G. G. C., & Vignali, C. 1997, *ApJ*, 478, 492

Carilli, C. L., et al. 2001, *ApJ*, 555, 625

Croom, S. M., Smith, R. J., Boyle, B. J., Shanks, T., Miller, L., Outram, P. J., & Loaring, N. S. 2004, *MNRAS*, 349, 1397

Dickey, J. M., & Lockman, F. J. 1990, *ARA&A*, 28, 215

Dietrich, M., Hamann, F., Shields, J. C., Constantin, A., Heidt, J., Jäger, K., Vestergaard, M., & Wagner, S. J. 2003, *ApJ*, 589, 722

Djorgovski, S. G., Gal, R. R., Odewahn, S. C., de Carvalho, R. R., Brunner, R., Longo, G., & Scaramella, R. 1998, *Wide Field Surveys in Cosmology*, 14th IAP meeting held May 26-30, 1998, Paris. Publisher: Editions Frontières. ISBN: 2-8 6332-241-9, p. 89, 89

Djorgovski, S. G., Stern, D., Mahabal, A. A., & Brunner, R. 2003, *ApJ*, 596, 67

Fabian, A. C., Celotti, A., Pooley, G., Iwasawa, K., Brandt, W. N., McMahon, R. G., & Hoenig, M. D. 1999, *MNRAS*, 308, L6

Fan, X., et al. 1999, *AJ*, 118, 1

Fan, X., et al. 2001, *AJ*, 121, 31

Fan, X., Narayan, V. K., Strauss, M. A., White, R. L., Becker, R. H., Pentericci, L., & Rix, H. 2002, *AJ*, 123, 1247

Fan, X., et al. 2003, *AJ*, 125, 1649

Farrah, D., Priddey, R., Wilman, R., Haehnelt, M., & McMahon, R. 2004, *ApJ*, 611, L13

Ferrero, E., & Brinkmann, W. 2003, *A&A*, 402, 465

Grupe, D., Mathur, S., Wilkes, B., & Elvis, M. 2004, *AJ*, 127, 1

Grupe, D., Mathur, S., Wilkes, B., & Osmer, P. 2005, *AJ*, submitted (astro-ph/0501521)

Guainazzi, M., et al. 1998, *A&A*, 339, 327

Hennawi, J. et al. 2005, *AJ*, submitted (astro-ph/0504535)

Ivezic, Z., et al. 2002, *AJ*, 124, 2364

Jansen, F., et al. 2001, *A&A*, 365, L1

Jiménez-Bailón, E., Piconcelli, E., Guainazzi, M., Schartel, N., Rodríguez-Pascual, P. M., & Santos-Lleó, M. 2005, *A&A*, 435, 449

Kaspi, S., Brandt, W. N., & Schneider, D. P. 2000, *AJ*, 119, 2031

Kellermann, K. I., Sramek, R., Schmidt, M., Shaffer, D. B., & Green, R. 1989, *AJ*, 98, 1195

Kirsch, M. G. F., et al. 2004, *Proc. SPIE*, 5488, 103

Laor, A., Fiore, F., Elvis, M., Wilkes, B. J., & McDowell, J. C. 1997, *ApJ*, 477, 93

Lyons, L. 1991, *Data Analysis for Physical Science Students* (Cambridge: Cambridge Univ. Press)

Maccacaro, T., Gioia, I. M., Wolter, A., Zamorani, G., & Stocke, J. T. 1988, *ApJ*, 326, 680

Maccarone, T. J., Gallo, E., & Fender, R. 2003, *MNRAS*, 345, L19

Magdziarz, P., & Zdziarski, A. A. 1995, *MNRAS*, 273, 837

Maiolino, R., Oliva, E., Ghinassi, F., Pedani, M., Mannucci, F., Mujica, R., & Juarez, Y. 2004, *A&A*, 420, 889

Manners, J., Almáni, O., & Lawrence, A. 2002, *MNRAS*, 330, 390

O'Neill, P. M., Nandra, K., Papadakis, I. E., & Turner, T. J. 2005, *MNRAS*, 358, 1405

Page, K. L., O'Brien, P. T., Reeves, J. N., & Turner, M. J. L. 2004a, *MNRAS*, 347, 316

Page, K. L., Reeves, J. N., O'Brien, P. T., Turner, M. J. L., & Worrall, D. M. 2004b, *MNRAS*, 353, 133

Paolillo, M., Schreier, E. J., Giacconi, R., Koekemoer, A. M., & Grogan, N. A. 2004, *ApJ*, 611, 93

Pentericci, L., et al. 2003, *A&A*, 410, 75

Petric, A. O., Carilli, C. L., Bertoldi, F., Fan, X., Cox, P., Strauss, M. A., Omont, A., & Schneider, D. P. 2003, *AJ*, 126, 15

Piconcelli, E., Jiménez-Bailón, E., Guainazzi, M., Schartel, N., Rodríguez-Pascual, P. M., & Santos-Lleó, M. 2005, *A&A*, 432, 15

Porquet, D., Reeves, J. N., O'Brien, P., & Brinkmann, W. 2004, *A&A*, 422, 85

Reynolds, C. S., & Nowak, M. A. 2003, *Phys. Rep.*, 377, 389

Richards, G. T., et al. 2002, *AJ*, 123, 2945

Schneider, D. P., Schmidt, M., & Gunn, J. E. 1989, *AJ*, 98, 1507

Schneider, D. P., et al. 2005, *AJ*, in press (astro-ph/0503679)

Schwartz, D. A., & Virani, S. N. 2004, *ApJ*, 615, L21

Snowden, S. L. 2002, in 'New Visions of the X-ray Universe in the XMM-Newton and Chandra Era', ESTEC Symposium, 26-30 November 2001 (astro-ph/0203311)

Spergel, D. N., et al. 2003, *ApJS*, 148, 175

Steffen, A. T., Barger, A. J., Cowie, L. L., Mushotzky, R. F., & Yang, Y. 2003, *ApJ*, 596, L23

Stern, D., Djorgovski, S. G., Perley, R. A., de Carvalho, R. R., & Wall, J. V. 2000, *AJ*, 119, 1526

Storrie-Lombardi, L. J., McMahon, R. G., Irwin, M. J., & Hazard, C. 1996, *ApJ*, 468, 121

Strateva, I., Brandt, W. N., Schneider, D. P., Vanden Berk, D., & Vignali, C. 2005, *AJ*, submitted (astro-ph/0503009)

Tananbaum, H., et al. 1979, *ApJ*, 234, L9

Vanden Berk, D., Yip, C., Connolly, A., Jester, S., & Stoughton, C. 2004, *ASP Conf. Ser.* 311: *AGN Physics with the Sloan Digital Sky Survey*, 311, 21

Vignali, C., Brandt, W. N., Fan, X., Gunn, J. E., Kaspi, S., Schneider, D. P., & Strauss, M. A. 2001, *AJ*, 122, 2143

Vignali, C., Bauer, F. E., Alexander, D. M., Brandt, W. N., Hornschemeier, A. E., Schneider, D. P., & Garmire, G. P. 2002, *ApJ*, 580, L105

Vignali, C., Brandt, W. N., Schneider, D. P., Garmire, G. P., & Kaspi, S. 2003a, *AJ*, 125, 418

Vignali, C., et al. 2003b, *AJ*, 125, 2876

Vignali, C., Brandt, W. N., Schneider, D. P., & Kaspi, S. 2005, *AJ*, 129, 2519

Walter, F., et al. 2003, *Nature*, 424, 406

Worsley, M. A., Fabian, A. C., Celotti, A., & Iwasawa, K. 2004a, *MNRAS*, 350, L67

Worsley, M. A., Fabian, A. C., Turner, A. K., Celotti, A., & Iwasawa, K. 2004b, *MNRAS*, 350, 207

Wilkes, B. J., & Elvis, M. 1987, *ApJ*, 323, 243

York, D. G., et al. 2000, *AJ*, 120, 1579